

Comprehensive Assignment of Mass Spectral Signatures from Individual *Bacillus atrophaeus* Spores in Matrix-Free Laser Desorption/Ionization Bioaerosol Mass Spectrometry

Abneesh Srivastava,[†] Maurice E. Pitesky,[†] Paul T. Steele,[†] Herbert J. Tobias,[†] David P. Fergenson,[†] Joanne M. Horn,[†] Scott C. Russell,[‡] Gregg A. Czerwieniec,[‡] Carlito B. Lebrilla,[‡] Eric E. Gard,[†] and Matthias Frank^{*,†}

Lawrence Livermore National Laboratory, Livermore, California 94550, and Department of Chemistry, University of California, Davis, California 95616

We have fully characterized the mass spectral signatures of individual *Bacillus atrophaeus* spores obtained using matrix-free laser desorption/ionization bioaerosol mass spectrometry (BAMS). Mass spectra of spores grown in unlabeled, ¹³C-labeled, and ¹⁵N-labeled growth media were used to determine the number of carbon and nitrogen atoms associated with each mass peak observed in mass spectra from positive and negative ions. To determine the parent ion structure associated with fragment ion peaks, the fragmentation patterns of several chemical standards were independently determined. Our results confirm prior assignments of dipicolinic acid, amino acids, and calcium complex ions made in the spore mass spectra. The identities of several previously unidentified mass peaks, key to the recognition of *Bacillus* spores by BAMS, have also been revealed. Specifically, a set of fragment peaks in the negative polarity is shown to be consistent with the fragmentation pattern of purine nucleobase-containing compounds. The identity of $m/z = +74$, a marker peak that helps discriminate *B. atrophaeus* from *Bacillus thuringiensis* spores grown in rich media is $[N_1C_4H_{12}]^+$. A probable precursor molecule for the $[N_1C_4H_{12}]^+$ ion observed in spore spectra is trimethylglycine ($^+N(CH_3)_3CH_2COOH$), which produces a $m/z = +74$ peak when ionized in the presence of dipicolinic acid. A clear assignment of all the mass peaks in the spectra from bacterial spores, as presented in this work, establishes their relationship to the spore chemical composition and facilitates the evaluation of the robustness of “marker” peaks. This is especially relevant for peaks that have been used to discriminate *Bacillus* spore species, *B. thuringiensis* and *B. atrophaeus*, in our previous studies.

Mass spectrometry provides a rapid detection method for the characterization of intact microorganisms.^{1,2} By integrating particle-

based analytical methods and mass spectrometry, a number of single-particle mass spectrometry techniques, such as laser-based RSMS,³ PALMS,⁴ RTAMS,⁵ ATOFMS,⁶ and LAMPAS^{7,8} and pyrolysis-based Py-MS⁹ and Py-GC-IMS,¹⁰ have emerged for the real-time analysis of individual atmospheric particles. The detection of single, micrometer-sized microorganism-containing particles is particularly relevant to the detection of pathogenic air-borne cells, such as aerosolized *Bacillus anthracis*. Consequently, it is not surprising that single-particle mass spectrometry is being actively developed for bioaerosol detection and identification by several groups.^{11–16} Among the laser-based desorption/ionization methods, two approaches exist. One utilizes the inherent advantages of matrix-assisted laser desorption/ionization mass spectrometry (MALDI-MS) to provide a soft ionization method for large biomolecules with the least amount of fragmentation for the

- (1) Fenselau, C.; Demirev, P. A. *Mass Spectrom. Rev.* **2001**, *20*, 157–171.
- (2) van Baar, B. L. M. *FEMS Microbiol. Rev.* **2000**, *24*, 193–219.
- (3) Johnston, M. V.; Wexler, A. S. *Anal. Chem.* **1995**, *67*, A721–726.
- (4) Murphy, D. M.; Thomson, D. S. *Aerosol Sci. Technol.* **1995**, *22*, 237–249.
- (5) Lazar, A.; Reilly, P. T. A.; Whitten, W. B.; Ramsey, J. M. *Environ. Sci. Technol.* **1999**, *33*, 3993–4001.
- (6) Gard, E.; Mayer, J. E.; Morrill, B. D.; Dienes, T.; Fergenson, D. P.; Prather, K. A. *Anal. Chem.* **1997**, *69*, 4083–4091.
- (7) Hinz, K. P.; Kaufmann, R.; Spengler, B. *Anal. Chem.* **1994**, *66*, 2071–2076.
- (8) Hinz, K. P.; Kaufmann, R.; Spengler, B. *Aerosol Sci. Technol.* **1996**, *24*, 233–242.
- (9) Goodacre, R.; Shann, B.; Gilbert, R. J.; Timmins, E. M.; McGovern, A. C.; Alsberg, B. K.; Kell, D. B.; Logan, N. A. *Anal. Chem.* **2000**, *72*, 119–127.
- (10) Snyder, A. P.; Thornton, S. N.; Dworzanski, J. P.; Meuzelaar, H. L. C. *Field Anal. Chem. Technol.* **1996**, *1*, 49–59.
- (11) Sinha, M. P.; Platz, R. M.; Vilker, V. L.; Friedlander, S. K. *Int. J. Mass Spectrom. Ion Processes* **1984**, *57*, 125–133.
- (12) Sinha, M. P.; Platz, R. M.; Friedlander, S. K.; Vilker, V. L. *Appl. Environ. Microbiol.* **1985**, *49*, 1366–1373.
- (13) Gieray, R. A.; Reilly, P. T. A.; Yang, M.; Whitten, W. B.; Ramsey, J. M. *J. Microbiol. Methods* **1997**, *29*, 191–199.
- (14) Parker, E. P.; Trahan, M. W.; Wagner, J. S.; Rosenthal, S. E.; Whitten, W. B.; Gieray, R. A.; Reilly, P. T. A.; Lazar, A. C.; Ramsey, J. M. *Field Anal. Chem. Technol.* **2000**, *4*, 31–42.
- (15) Stowers, M. A.; van Wuijckhuijse, A. L.; Marijnissen, J. C. M.; Scarlett, B.; van Baar, B. L. M.; Kientz, C. E. *Rapid Commun. Mass Spectrom.* **2000**, *14*, 829–833.
- (16) Fergenson, D. P.; Pitesky, M. E.; Tobias, H. J.; Steele, P. T.; Czerwieniec, G. A.; Russell, S. C.; Lebrilla, C. B.; Horn, J. M.; Coffee, K. R.; Srivastava, A.; Pillai, S. P.; Shih, M. T. P.; Hall, H. L.; Ramponi, A. J.; Chang, J. T.; Langlois, R. G.; Estacio, P. L.; Hadley, R. T.; Frank, M.; Gard, E. E. *Anal. Chem.* **2004**, *76*, 373–378.

* Corresponding author. E-mail: frank1@llnl.gov. Tel: 925-423-5068. Fax: 925-424-2778.

[†] Lawrence Livermore National Laboratory.

[‡] University of California.

detection of biomarkers with large molecular mass.^{1,2,15,17–19} In single-particle MALDI-MS, a matrix is added online to coat the bioaerosol of interest. In demonstration of online matrix addition to bioaerosol detection, Stowers et al.¹⁵ have used a 308-nm laser on *Bacillus atrophaeus* spores coated with a matrix of picolinic acid or sinapinic acid to produce an ion peak at $m/z = +1224$ Da. This peak has been attributed to cortex peptidoglycan.

In the second approach that has been pursued by our group,¹⁶ a matrix-free laser desorption/ionization bioaerosol mass spectrometry (BAMS) method is utilized to fully eliminate the need for reagents and sample preparation, which can impede in situ real-time particle analysis. BAMS has been demonstrated¹⁶ to provide real-time chemical differentiation of individual *Bacillus thuringiensis* and *B. atrophaeus* spores from one another very accurately and rapidly within seconds. The observed mass peaks are mainly at low mass ($|m/z| \leq 200$ Da), presumably due to limitations in the ionization process and the mass spectrometer. Limits in high mass sensitivity due to low ion transmission have been identified and are being removed from the next-generation BAMS.²⁰ Typical mass spectral patterns consist of peaks at characteristic m/z , but show variations in peak intensities. Such variations are in part due to inhomogeneities in the laser profile, as demonstrated by Steele et al.²¹ Nonetheless, an examination of averaged spore spectra allows unambiguous identification of the prominent peaks, some of which have been tentatively assigned based on previous isotope labeling studies.²² Here we provide a complete identification of the features in the spore spectra that includes many previously unidentified peaks. The studies presented here provide a comprehensive comparison of mass spectral signatures for bacterial spores grown in ¹³C and ¹⁵N isotopically labeled media with that of spores grown in unlabeled media. In the event of fragment ions losing more than one functional group (e.g., HCN and NH₃), we have measured standards to reproduce the observed fragment and the lost functional group (HCN, NH₃) to make a cogent assignment. In addition, standards were measured in the presence of dipicolinic acid, which is known to be present in spores and may act as an internal matrix, for the assignment of other fragment ions.

EXPERIMENTAL SECTION

Spore Preparation. *B. atrophaeus*, previously known as *B. subtilis var niger* or *Bacillus globigii* (ATCC 9372, Dugway Proving Ground, Dugway, UT), cells were grown to midlog phase in BioExpress cell growth media (Cambridge Isotopes) and then aliquoted in a 1:25 dilution into 75 mL of BioExpress media. The *Bacillus* sporulated in BioExpress sporulation media in a shaker incubator at 32 °C until ~90% of all the cells were refractile (3–4 days). Three such sample sets were made in BioExpress unlabeled, ¹³C-labeled (98%), and ¹⁵N-labeled (98%) cell growth media.

Phase contrast microscopy using a Zeiss phase contrast microscope and spore staining were used to confirm the presence of bacterial spores. Spores were harvested by centrifugation at 8000g for 10 min and washed in sterilized double-distilled water. After being washed two times, the spores were reconstituted in double-distilled water at concentrations of ~10⁸ spores/mL as determined using a Petroff–Hauser counting chamber.

Aerosol Generation. The spore solution was aerosolized from a solution concentration of ~10⁶/mL using a Collison nebulizer with a 1.0–1.5 L/min flow of clean, dry air. The wet bioaerosol was dried with a diffusion drier containing activated silica gel desiccant and was then passed through copper tubing to the aerosol mass spectrometer inlet. The mean aerodynamic diameter ± 1 standard deviation of the aerosol particles at the inlet was determined by aerodynamic sizing to be 0.96 ± 0.09 , 0.99 ± 0.09 , and $0.91 \pm 0.11 \mu\text{m}$ for spores grown in unlabeled and ¹³C- and ¹⁵N-labeled growth media. (The aerodynamic diameter d_a is defined as the diameter of the unit density, $\rho_p = 1 \text{ g/cm}^3$, sphere that has the same settling velocity as the particle.²³ These measured aerodynamic sizes are consistent with our earlier reports¹⁶ as well as with the aerodynamic size reported for single spores.^{24,25} The physical shape and dimension of spore is rodlike of $1.25 \times 0.75 \mu\text{m}$ ²⁶ and density of 1.45 g cm^{-3} .²⁷

Aerosol generation is conducted in a biological safety class II (Baker Co.) cabinet, and aerosolized spores are directly introduced into the BAMS through a closed copper tubing without any dispersal in the laboratory room. The vacuum pump exhausts of the BAMS system are filtered by HEPA filters. Routine cleaning of nozzle and skimmer sections of BAMS is done for decontamination.

Aerosol Time-of-Flight Spectrometer. The BAMS system is based on a modified TSI ATOFMS (model 3800) that is being developed for bioaerosol laser desorption/ionization mass spectrometry in our group.¹⁶ An illustration can be found in Gard et al.⁶ Briefly, dried aerosols at atmospheric pressure are sampled via a 340- μm -diameter nozzle into the first stage of the mass spectrometer vacuum system, maintained at a pressure of ~2.4 Torr. The particles then pass through two skimmers into a particle sizing region at ~10⁻⁴ Torr.

The size of entrained aerosol particles is determined by aerodynamic sizing in the following way. The velocity of a particle is determined by measuring its transit time between two vertically offset, orthogonally positioned “sizing” laser beams (continuous-wave 532 nm). This arrangement of the lasers ensures that only particles that travel straight down the center of the instrument are sized and counted. As a particle crosses the sizing laser beams two scattered light signals separated by the particle transit time are produced and detected using photomultiplier tubes. The aerodynamic size of the particle is obtained by using a conversion from measured velocity to aerodynamic diameter. This conversion

(17) Lay, J. O. *Mass Spectrom. Rev.* **2001**, *20*, 172–194.

(18) He, L.; Murray, K. K. *J. Mass Spectrom.* **1999**, *34*, 909–914.

(19) Jackson, S. N.; Murray, K. K. *Anal. Chem.* **2002**, *74*, 4841–4844.

(20) Russell, S. C.; Czerwieniec, G.; Lebrilla, C.; Tobias, H.; Fergenson, D. P.; Steele, P.; Pitesky, M.; Horn, J.; Srivastava, A.; Frank, M.; Gard, E. E. Manuscript in preparation.

(21) Steele, P. T.; Tobias, H. J.; Fergenson, D. P.; Pitesky, M. E.; Horn, J. M.; Czerwieniec, G. A.; Russell, S. C.; Lebrilla, C. B.; Gard, E. E.; Frank, M. *Anal. Chem.* **2003**, *75*, 5480–5487.

(22) Czerwieniec, G.; Russell, S. C.; Tobias, H. J.; Pitesky, M. E.; Fergenson, D. P.; Steele, P. T.; Srivastava, A.; Horn, J. M.; Frank, M.; Gard, E. E.; Lebrilla, C. B. *Anal. Chem.* **2005**, *77*, 1081–1087.

(23) Hinds, W. C. *Aerosol Technology*, 1st ed.; John Wiley & Sons: New York, 1982.

(24) Wang, H.; Reponen, T. A.; Adhikari, A.; Willeke, K. *Aerosol Sci. Technol.* **2004**, *38*, 1139–1148.

(25) Pan, Y. L.; Aptowicz, K. B.; Chang, R. K.; Hart, M.; Eversole, J. D. *Opt. Lett.* **2003**, *28*, 589–591.

(26) Hitchins, A. D.; Gould, G. W.; Hurst, A. J. *Gen. Microbiol.* **1963**, *30*, 445–453.

(27) Beaman, T. C.; Greenamyre, J. T.; Corner, T. R.; Pankratz, H. S.; Gerhardt, P. *J. Bacteriol.* **1982**, *150*, 870–877.

is based on an accurate size calibration determined using monodisperse polystyrene latex beads of known sizes. A trigger pulse based on the particle's velocity is then used to trigger the desorption/ionization (D/I) laser to hit the particle when it arrives in the ion source region of the mass spectrometer. The base pressure in the source region is $\sim 10^{-7}$ Torr during data collection. The D/I laser is a frequency-quadrupled Q-switched Nd:YAG (Ultra CFR, Big Sky Laser Technologies, Inc.) laser emitting 266-nm radiation with a near-Gaussian profile and ~ 5 -ns pulse width. The laser pulse energy is attenuated using a half-wave plate and polarizer and focused into the ion source using a 10-cm focal length, plano-convex lens. Beam profile measurements (using a Spiricon Pyrocam III camera) give a laser beam size of ~ 400 μm (fwhm) in the center plane of the ion source. The average laser pulse energy is 0.22 mJ. The laser pulse energy is chosen to be consistent with prior results,^{16,21} determined to be optimal for *B. atrophaeus* spores. The choice of optimal laser fluence settings was based on minimal fragmentation and reasonable hit rate ($\sim 15\%$), where hit rate is the fraction of tracked particles that produce a measurable mass spectrum. The overall efficiency of this early BAMS prototype was relatively low. Only about 1 in 1000 particles sampled into this instrument was hit and produced a measurable mass spectrum. This efficiency has since been improved significantly. A full description of the laser fluence dependence of *Bacillus* spores can be found in Steele et al.²¹ Positive and negative ions that are generated by the laser desorption/ionization from an aerosol particle are extracted in opposite directions using a dual-polarity reflectron time-of-flight spectrometer to two separate microchannel plate detectors, one each for positive and negative ion detection. The detector ion signals are sampled at 500 MHz by a four-channel Cougar digitizer running in extended dynamic range mode (two channels per polarity) for the positive and negative ions. The raw data are analyzed using data import and analysis software developed by our group. An autocalibration method is used to correct for shot-to-shot jitter in the time-of-flight spectra. In this method, an algorithm is used to calibrate each data spectrum individually.²¹

Typically 100–500 spectra were collected per sample. In addition to *Bacillus* spores, the mass fragmentation patterns of a number of chemical standards were also studied. The average laser pulse energy employed for study of standards was 100 μJ . All chemicals used were obtained from Sigma-Aldrich, Inc. at the highest available purity. Nucleobase-containing compounds studied were adenine, adenosine, adenosine 5'-monophosphate sodium salt, adenosine 5'-diphosphate sodium salt, adenosine 5'-triphosphate sodium salt, cytidine, cytidine monophosphate, cytidine diphosphate, guanosine, guanosine 5'-diphosphate sodium salt, guanosine 5'-triphosphate sodium salt, β -nicotinamide adenine dinucleotide reduced dipotassium salt, and DNA (type XIV, from herring testes, as the sodium salt). In addition trimethylglycine (betaine) and dipicolinic acid (1,6-pyridinedicarboxylic acid, DPA) standards and mixture were also studied.

RESULTS AND DISCUSSION

Averages of the mass spectra of individual *B. atrophaeus* spore particles are shown in Figure 1 for spores grown in unlabeled (a), ¹⁵N-labeled (b), and ¹³C-labeled (c) Bioexpress cell growth media, respectively. The total number of spectra shown in Figure 1a–c is 324, 420, and 125. Figure 2 a1, b1, and c1 show expanded

regions of Figure 1a, b, and c from $m/z = -185$ to -85 while Figure 2a2, b2, and c2 show expanded regions from $m/z = +55$ to $+95$ of the same spectra as in Figure 1a, b, and c. Although we collected spectra from individual spores, average spectra are used to characterize the spore mass signatures. Averaging reduces the variations observed at the single-spectrum level specifically due to laser fluences.²¹ Thus average spectra are more representative of the general spore mass signatures. The overall spore mass signatures were similar to that obtained from spores grown in ^{1/4} TY and G media, reported in a recent publication.¹⁶ The mass peaks observed are in the 200 Da range for both positive and negative ions and are classified below under separate chemical groups.

Metal Ions. Metal ions, such as Na^+ and K^+ , are easily identifiable in the spore spectra at $m/z = +23$, $+39$, and $+41$ for labeled and unlabeled growth media and account for the largest ion peaks in the positive ion spectrum. A set of ion peaks observed at $m/z = +57$, $+66$, and $+82$ are found to be consistent with calcium ion complexes $[\text{CaOH}]^+$, $[\text{CaCN}]^+$, and $[\text{CaCNO}]^+$, based on their number of carbon and nitrogen shifts in the spore mass spectrum. Assignment of these ions as calcium adducts is deduced from the known high calcium content of *Bacillus subtilis* spores. We do not observe any peak at $m/z = +20$ that would correspond to the free Ca^{2+} ion and only observe peaks that correspond to bound Ca^{2+} as in $[\text{CaOH}]^+$, $[\text{CaCN}]^+$, and $[\text{CaCNO}]^+$. A peak at $m/z = 40$ in the BAMS mass spectra for spores grown in unlabeled media is seen to be invariant in both ¹⁵N-labeled, and ¹³C-labeled media grown spores. This is tentatively assigned to Ca^+ monovalent ion. In addition to calcium, the predominant divalent ion found in spores,²⁸ magnesium and manganese are also present at elevated concentrations inside a spore²⁹ and together with calcium can comprise up to 3% of the dry weight of the spore.³⁰ However, ion peaks for magnesium or manganese either as free or bound divalent ion are absent in the BAMS spore spectra.

Dipicolinic Acid. Peaks observed at $m/z = -166$ and -167 are assigned to DPA ($\text{C}_7\text{H}_5\text{NO}_4$). This assignment is based on observed shifts of one mass unit in ¹⁵N-labeled media and seven mass units in the ¹³C-labeled media as seen in Figure 2b1 and c1, respectively, compared to Figure 2a1. Electron capture negative ion mass spectrometry data of dipicolinic acid show³¹ a strong M^- peak at -167 at relatively low energy, 0.3 eV. Ion molecule reactions between low-energy electrons, presumably created from the laser–spore interaction, and neutral DPA molecules would account for the DPA-related $m/z = -167$ ion in the spore mass spectra. The presence of $m/z = -166$ in the spore mass spectra is indicative of loss of a proton from one of the two carboxylic acid groups (COOH) present in DPA. Further evidence of the presence of DPA in the spore mass spectra is seen from the assignment of the $m/z = -122$ peak. Observed mass shifts of six units in the ¹⁵N-labeled spectra and of one unit in the ¹³C-labeled spectra, as seen in Figure 2b1 and c1, respectively, compared to Figure 2a1, match the number of nitrogen and carbon atoms present in $\text{C}_6\text{H}_4\text{NO}_3^-$ ($m/z = -122$) that would result from the

(28) Perry, J. J.; Foster, J. W. *J. Bacteriol.* **1956**, *72*, 295–300.

(29) Murrell, W. G.; Warth, A. D. In *Spores III*; Campbell, L. L., Halvorson, O., Eds.; American Society for Microbiology: Ann Arbor, MI, 1965; pp 1–24.

(30) Young, E.; Fitz-James, P. C. *J. Cell Biol.* **1962**, *12*, 115–133.

(31) Beverly, M. B.; Voorhees, K. J.; Hadfield, T. L.; Cody, R. B. *Anal. Chem.* **2000**, *72*, 2428–2432.

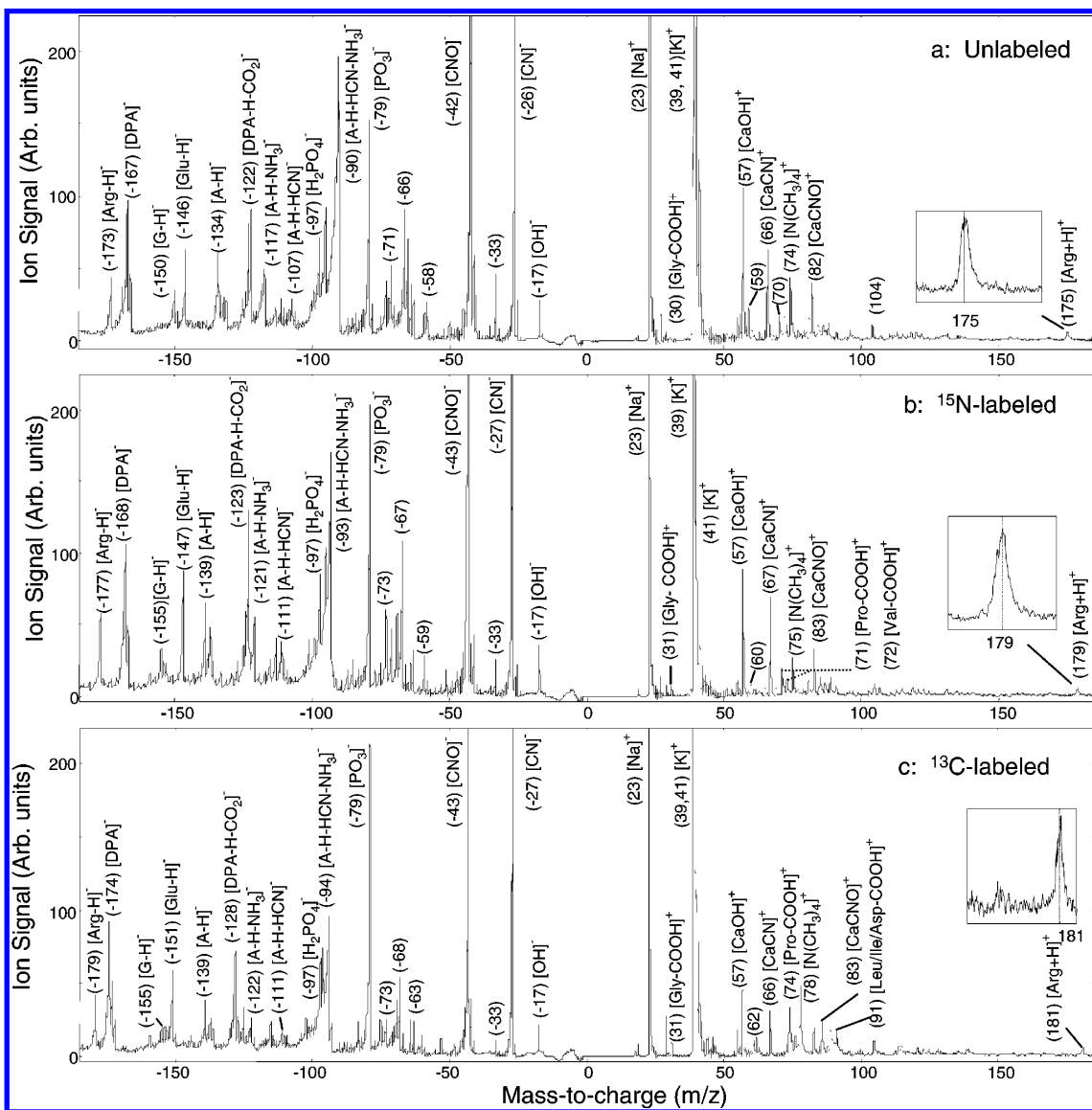


Figure 1. Dual polarity average mass spectra of *B. atrophaeus* spore (a–c: 324, 420, and 125 spectra, respectively) grown in unlabeled (a), ^{15}N -labeled (b), and ^{13}C -labeled (c) Bioexpress growth media. The inset in each panel shows the protonated arginine peak.

loss of a CO_2 group from the deprotonated DPA ion. Both $m/z = -166$ and -122 peaks are also observed in the mass spectra of the pure DPA standard and further support our final assignments of $\text{DPA}(\text{C}_7\text{H}_4\text{NO}_4^-)$ and its fragment ($\text{C}_6\text{H}_4\text{NO}_3^-$) ion.

Amino Acids. Two prominent peaks observed in the spore negative spectra are found at $m/z = -173$ and -146 . As can be seen from Figures 1 and 2, these peaks show a clear shift to -179 and -151 in the ^{13}C -labeled media and to -177 and -147 in the ^{15}N -labeled media, respectively. The peak assignments inferred from these shifts are consistent with deprotonated arginine ($\text{C}_6\text{H}_{13}\text{N}_4\text{O}_2^-$) and glutamic acid ($\text{C}_5\text{H}_8\text{NO}_4^-$), respectively. These assignments also agree with assignments made previously for BAMS spectra for spores grown in $1/4$ TY media,¹⁶ G media,¹⁶ and LB media.²²

Another prominent peak in the positive polarity appears at $m/z = +175$ in the unlabeled case and shifts to $m/z = +179$ for ^{15}N -labeled media and $m/z = +181$ for ^{13}C -labeled media. This suggests the peak at $m/z = +175$ arises from protonated arginine, $[\text{C}_6\text{H}_{14}\text{N}_4\text{O}_2 + \text{H}]^+$.

The presence of glutamic acid and arginine in the spore spectra is consistent with the reported composition of spore amino acid pools. The very high levels of L-glutamate and L-arginine in *B. subtilis* represent intracellular concentrations of the order of 0.1 M.³² This is equivalent to $\sim 10^7$ molecules/spore. In contrast, the concentrations of other free amino acids are only 5% of the total pool reported for *B. subtilis* grown in supplemented nutrient broth. Both arginine and glutamic acid when measured as pure aerosol standards yield a deprotonated and protonated peak.^{22,33} However, no evidence of a protonated glutamate peak is seen in the spore spectrum. In the case of arginine, a small contribution from protonated parent ion is observed (see Figure 1). This result is possibly linked to differences in gas-phase basicities (arginine 236 kcal/mol³⁴ and glutamic acid 209 kcal/mol³⁴) of the two amino

(32) Nelson, D. L.; A., K. *J. Biol. Chem.* **1970**, *245*, 1128–1136.

(33) Russell, S. C.; Czerwieniec, G.; Lebrilla, C.; Tobias, H.; Fergenson, D. P.; Steele, P.; Pitesky, M.; Horn, J.; Srivastava, A.; Frank, M.; Gard, E. E. *J. Am. Soc. Mass Spectrom.* **2004**, *15*, 900–909.

(34) Carr, S. R.; Cassady, C. J. *J. Mass Spectrom.* **1997**, *32*, 959–967.

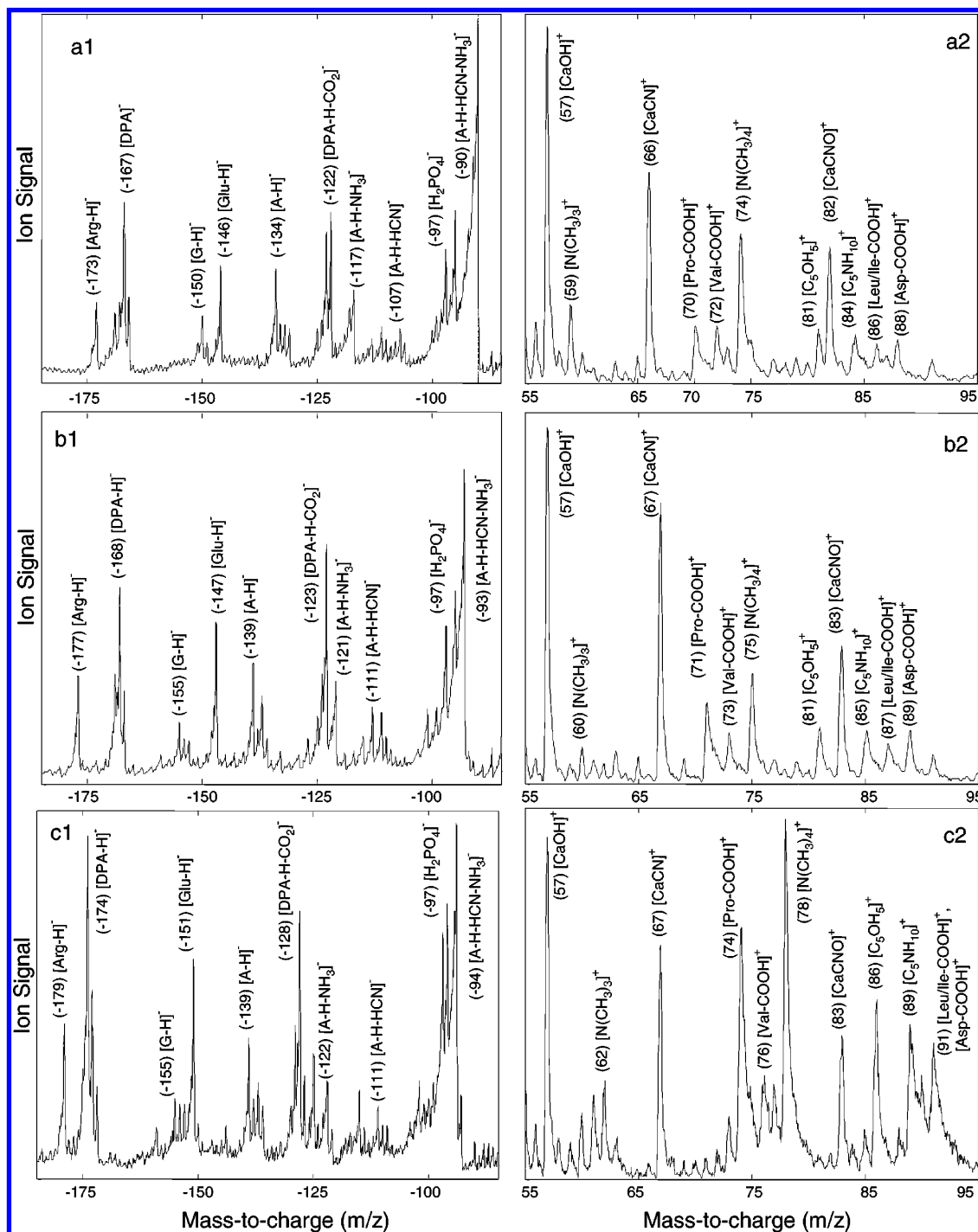


Figure 2. Expanded mass spectral regions of *B. atrophaeus* spore spectra shown in Figure 1, for spores grown in unlabeled (a1, a2), ^{15}N -labeled (b1, b2), and ^{13}C -labeled (c1, c2) Bioexpress growth media. Two mass ranges are shown, -185 to -85 (see a1, b1, and c1) on the left and $+55$ to $+95$ (see a2, b2, and c2) on the right. All other details are same as Figure 1. See text for discussion.

acids favoring a proton transfer from the glutamic acid to arginine in the plume. BAMS studies of standard 1:1 mixtures of arginine/glutamic acid have been shown to favor protonation of arginine over glutamic acid.³³ Additionally, in the presence of dipicolinic acid the effective ionization probability of arginine and glutamic acid has been shown to increase by as much as 1 order of magnitude.³³ These results suggest that the two amino acids are in proximity in the spore, probably in the core along with dipicolinic acid, favoring ion formation. Strong ternary complexes of DPA, Ca^{2+} , and amino acids do exist,^{35,36} and a similar network

might exist in the spore core. Such a close arrangement would favor effective ionization of the amino acids and allow for proton transfer between glutamate and arginine.

Distinct lower intensity peaks are present in average spectra from positive ions (see Figures 1 and 2). These have mass-to-charge ratios of $+30$, $+70$, $+72$, $+86$, and $+88$ and are seen to shift by one mass unit to $m/z = +31$, $+71$, $+73$, $+87$, and $+89$ for the ^{15}N -labeled media and by 1, 4, 4, 5, and 3 units to $m/z =$

(35) Young, I. E. *Can. J. Microbiol.* **1959**, *5*, 197–202.

(36) Tang, T.; Rajan, K. S.; Grecz, N. *Biophys. J.* **1968**, *8*, 1458–1474.

+31, +74, +76, +91, and +91 for the ^{13}C -labeled media. This result is consistent with a set of amino acids that have lost the carboxyl group from the deprotonated parent ion (a loss of 45 mass units). The assignments obtained for $m/z = +30, +70, +72, +86,$ and $+88$ are shown in Figure 1 and are consistent with the loss of a COOH group from glycine, proline, valine, leucine/isoleucine, and aspartic acid. The presence of fragmented amino acid peaks in the positive ion spectrum suggests the presence of glycine, proline, valine, leucine/isoleucine, and aspartic acid in small amounts in the spores. In contrast, a vegetative cell BAMS mass spectrum²² has significantly higher ion signals from decarboxylated amino acids.

Additional peaks from positive ions at $m/z = +81$ and $+84$ are present close to the fragmented amino acid peaks. These peaks shift to $m/z = +81, +86$ and $+84,$ and $+89$ for ^{15}N -labeled and ^{13}C -labeled growth media as shown in Figure 2. Tentative assignments are thus C_5OH_5^+ and $\text{C}_5\text{NH}_{10}^+$, respectively.

Phosphates. Peaks observed at $m/z = -79$ and -97 in the spore spectra are assigned to PO_3^- and H_2PO_4^- ions. Those peaks do not show an isotopic shift in ^{15}N -labeled and ^{13}C -labeled media, as is expected for those ions. Mass peaks at $m/z = -79$ and -97 are commonly found in mass spectra of phosphate-related compounds. About 45% of the total phosphorus content in *B. subtilis* spores is in nucleic acids.³⁷ Our results with DNA and free nucleotide standards confirm the expected presence of phosphate fragments at $m/z = -79$ and -97 and support their assignments as PO_3^- and H_2PO_4^- ions in the spore spectra.

Purine Nucleobases. The origin of $m/z = -134$ in the spore spectra obtained using BAMS has been unclear. It was tentatively assigned to aspartic acid¹⁶ as well as potentially linked to DPA complex with Ca^{2+} ion based on desorption/ionization studies with DPA/ $\text{Ca}(\text{OH})_2$ aerosol mixture.²² Here we provide a more direct assignment based on observed isotopic shifts. We have unambiguously identified the molecular formula for $m/z = -134$ to be $\text{C}_5\text{N}_5\text{H}_4^-$. The assignment is depicted in Figure 2 as $m/z = -134,$ $-139,$ and -139 in unlabeled, ^{15}N -labeled, and ^{13}C -labeled media, respectively. Furthermore, $m/z = -117, -107,$ and -90 have been assigned as $\text{C}_5\text{N}_4\text{H}_1^-, \text{C}_4\text{N}_4\text{H}_3^-,$ and C_4N_3^- based on isotopic shifts to $m/z = -121, -111,$ and -93 in ^{15}N -labeled media and $m/z = -122, -111,$ and -94 in ^{13}C -labeled media are seen in Figure 2b1 and c1, respectively, compared to Figure 2a1. These assignments indicate a nitrogen-rich moiety. Consequently, this assignment rules out aspartic acid ($\text{C}_4\text{H}_7\text{NO}_4$), which has only one nitrogen atom, as well as any kind of fragment from a DPA complex with calcium hydroxide, $(\text{C}_7\text{H}_5\text{NO}_4)\text{Ca}(\text{OH})_2$, which would also have only one nitrogen atom. Based on the high number of nitrogen atoms it is likely that $m/z = -134, -117, -107,$ and -90 are related to a common parent molecular structure. The assignment of $m/z = -134$ as $\text{C}_5\text{N}_5\text{H}_4^-$ is found to be consistent with deprotonated adenine, found in free nucleotides, nucleic acids, and several coenzymes. To probe the relationship between $m/z = -134, -117, -107,$ and -90 and adenine, we examined the mass fragmentation pattern of pure adenine standard under our aerosolization and laser desorption/ionization conditions. The spectrum for adenine is shown in Figure 3. In the negative polarity, $m/z = -134, -117, -107, -90,$ and -65 are clearly observed. This set of peaks is also observed in the *Bacillus* spore spectrum for the unlabeled

case. In addition to adenine, we have also examined the mass fragmentation pattern of several adenine (A)-, guanine (G)-, and cytosine (C)-containing nucleosides, mono-, di-, and triphosphate nucleotides, coenzyme, and DNA. Representative spectra for guanosine 5'-diphosphate sodium salt and cytidine are shown along with adenine in Figure 3. Our studies with seven adenine-containing molecules listed in the Experimental Section produced $m/z = -134, -117, -107, -90$ and -65 fragment peaks in all the mass spectra. Guanine containing molecules were found to give rise to $m/z = -150, -133, -106,$ and -90 . In contrast, cytidine exhibits peaks at $m/z = -110, -95, -84,$ and -67 that do not overlap with $m/z = -134, -117, -107,$ and -90 . This result indicates that $m/z = -134, -117, -107,$ and -90 in the spore spectra largely arise from adenine-containing molecules while guanine and its derivatives can also contribute to $m/z = -90$. We also see evidence of the deprotonated guanine ion in the spore spectrum at $m/z = -150$. This is depicted in Figure 2 as $\text{C}_5\text{N}_5\text{OH}_4^-$ ion at $m/z = -150, -155,$ and -155 for unlabeled, ^{15}N -labeled, and ^{13}C -labeled media, respectively.

The isotopic assignment for the observed fragmentation pattern of $m/z = -134, -117, -107,$ and $-90,$ as $\text{C}_5\text{N}_5\text{H}_4^-, \text{C}_5\text{N}_4\text{H}_1^-, \text{C}_4\text{N}_4\text{H}_3^-,$ and C_4N_3^- , is consistent with adenine-H, adenine-H - NH_3 , adenine-H - HCN , and adenine-H - $\text{HCN} - \text{NH}_3$ anions. The deprotonated ion, $m/z = -134$, probably involves loss of the pyrrole hydrogen based on calculated gas-phase acidities for the most acidic hydrogen site.³⁸ The dissociation pathway for the deprotonated adenine appears to involve loss of NH_3 , loss of HCN , and loss of NH_3 and HCN . The possible reaction mechanism likely involves the pyrimidine ring opening. Assignment of $m/z = -65$ is tentatively $\text{C}_3\text{N}_2\text{H}^-$ based on observed shifts in the spore spectra.

The relative contribution of different adenine sources within a spore to its observed mass spectrum cannot be quantified in this work. However, a comparison of typical concentrations of a few key sources such as free adenine nucleotides, i.e., AMP, ADP, ATP, adenine-containing co-enzymes, i.e., NAD, NADP, FAD, and nucleic acids, i.e., RNA and DNA, can be made for some understanding of their relative contributions. It is estimated that the number of free adenine nucleotides and coenzymes is $\sim 10^5$ and $\sim 10^4$ molecules/cell,³⁹ respectively. The contribution of DNA and RNA in relative comparison is in the $\sim 10^8$ – 10^9 nucleobase/cell range. This would suggest adenine mostly arises from DNA/RNA. However, the ionization efficiencies and subsequent fragmentation to form adenine would be strongly dependent on the size of the molecule. As an example, a comparison of AMP versus ATP mass spectrum acquired by BAMS at different laser fluences indicates lower ionization efficiency for ATP compared to AMP, as the size of the molecule increases by two phosphate groups. The total ion signal for $m/z = -134$ and its fragments ions obtained for ATP in our studies (data not shown) is $\sim 5\times$ lower in comparison to AMP at 0.2 mJ laser pulse energy for a $\sim 400\text{-}\mu\text{m}$ fwhm beam. Fragmentation of DNA/RNA would similarly be expected to be less efficient in producing adenine and its fragment peaks based on its larger size.

It is interesting to point that although the level of total adenine nucleotide is similar in spores and cells the relative concentration

(37) Nelson, D. L.; Kornberg, A. *J. Biol. Chem.* **1970**, *245*, 1137–1145.

(38) Rodgers, M. T.; Campbell, S.; Marzluff, E. M.; Beauchamp, J. L. *Int. J. Mass Spectrom. Ion Processes* **1994**, *137*, 121–149.

(39) Setlow, P.; Kornberg, A. *J. Biol. Chem.* **1970**, *245*, 3637–3644.

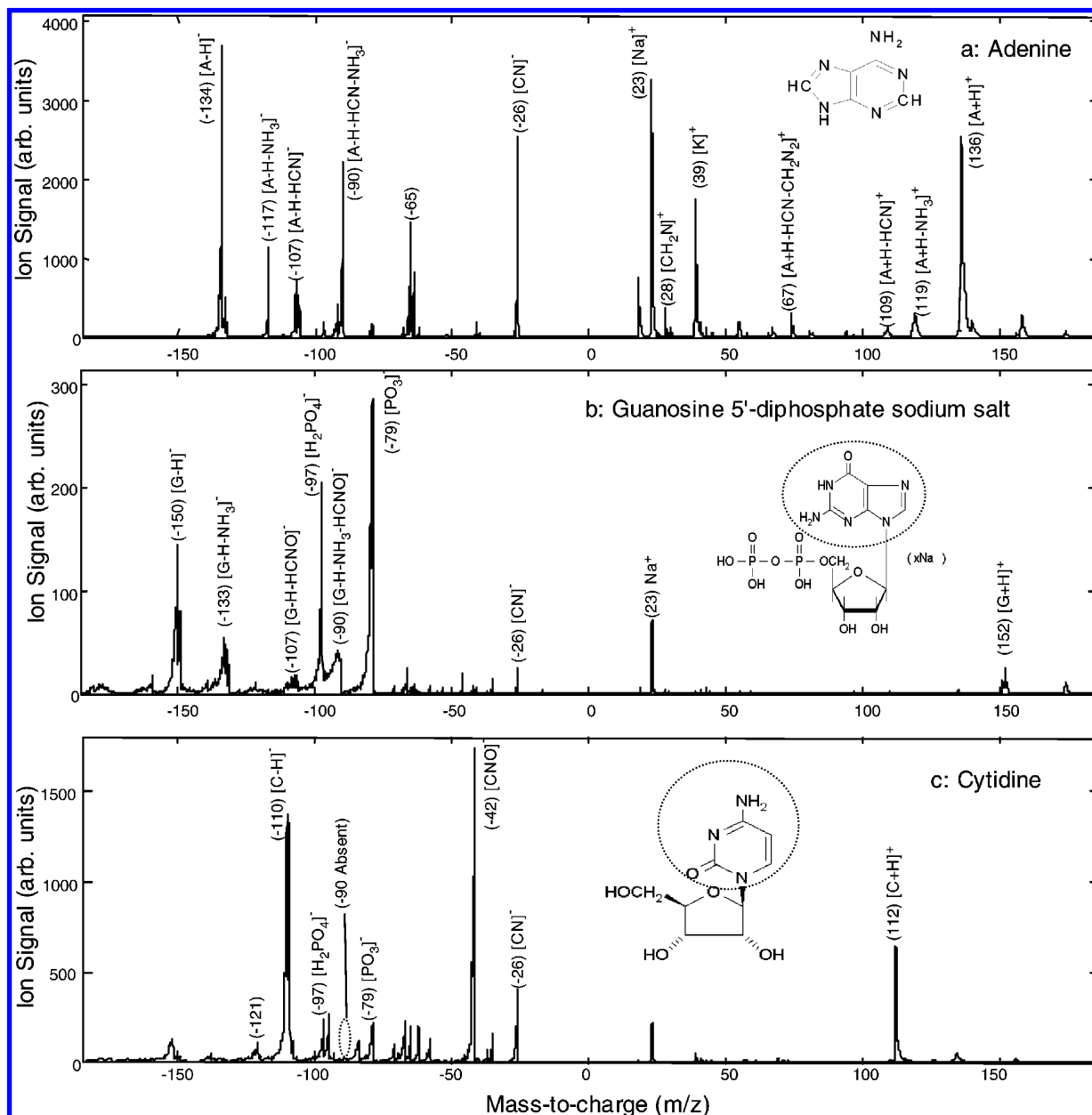


Figure 3. Dual polarity average mass spectra (200 spectra each) of nucleobase containing standards, namely, adenine (A), guanosine 5'-diphosphate sodium salt (GDP), and cytidine. Spectra were obtained at 100 μJ average laser pulse energy. The encircled chemical structures in each figure represent the nucleobase substructures adenine (A), guanine (G), and cytosine (C), respectively. Note presence of $m/z = -134$, -117 , -107 , and -90 fragment ions in adenine mass spectra, similar to that found in spore spectra.

of AMP to ATP is substantially higher in spores. For example, in *Bacillus megaterium* the ATP/(ADP+AMP) ratio is 0.22:1 and in cells 3.7:1³⁹ with similar findings for *B. subtilis* and *Bacillus cereus* spores. This would suggest a higher adenine-related signal in spores relative to vegetative cell and might explain the near absence of $m/z = -134$, -90 in the vegetative cell BAMS mass spectrum.²²

Also confirmed is the assignment of $m/z = -17$, -26 , and -42 as OH^- , CN^- , and CNO^- based on observed mass shifts of 0, 1, and 1 for the ^{15}N -labeled and the ^{13}C -labeled media. CN^- and CNO^- along with PO_3^- contribute the largest ion signal in the negative spectrum. As can be seen from spectra shown in Figure 3, nucleobases can contribute to the CN^- and CNO^- ions seen in the spore spectra.

At 0.22 mJ laser pulse energy, overall fragmentation of adenine was similar to that reported in Figure 3a for 100 μJ but with higher ion signal at $m/z = -26$. The presence of $m/z = +23$ and $+39$ in the adenine spectra is attributed to Na^+ and K^+ ions in the nebulizer solution. The absence of a $m/z = 136$ peak in the spore spectra might in part be related to the presence of large adenine-containing moieties in the spore that produce smaller $m/z = 136$ signal compared to pure adenine.

Trimethylglycine (Betaine). For $m/z = 74$ our isotope labeling results indicate a shift to $m/z = +75$ in ^{15}N -labeled media and $m/z = +78$ in ^{13}C -labeled media; see Figure 2. This result is consistent with $^+\text{N}(\text{CH}_3)_4$ as well as protonated amines. However, there is no evidence in the literature of free amines being present in spores. Quaternary ammonium salts, of the kind $^+\text{N}(\text{CH}_3)_4 \text{X}^-$,

where X^- is a negative ion, such as halide, sulfate, or phosphate, are also absent from the growth media. As there is no evidence for ${}^+N(CH_3)_4$ to be present in the media or within the spore it is probably a fragment of a ${}^+N(CH_3)_3CH_2$ -containing moiety, such as choline (${}^+N(CH_3)_3CH_2CH_2OH$), the phosphocholine (PC) headgroup of a phospholipid (${}^+N(CH_3)_3CH_2CH_2OP(O)_2OCH_2$), or trimethylglycine (${}^+N(CH_3)_3CH_2COOH$). It is unlikely for a PC-containing phospholipid to be the source of the observed $m/z = +74$ fragment peak based on known lipid concentrations in *B. subtilis*. Nearly 70% of *B. subtilis* membrane lipids are in the neutral lipid fraction,⁴⁰ of which phosphatidylglycerol ($CH_2(OH)CH_2(OH)CH_2OP(O^-)(O)OCH_2CH-R(R')$) is the major constituent at 70% and phosphatidylethanolamine (${}^+(H)N(CH_3)_2CH_2CH_2OP(O^-)(O)OCH_2CH-R(R')$) is minor at 12% with no detectable amounts of phosphatidylcholine (${}^+(H)N(CH_3)_3CH_2CH_2OP(O^-)(O)OCH_2CH-R(R')$). Here $R(R')$ denotes the fatty acid chain of the phospholipid. In addition, we also analyzed pure standard of dioleoylphosphatidylcholine by BAMS and did not observe a $m/z = +74$ fragmentation peak. However, the possibility of trimethylglycine, ${}^+N(CH_3)_3CH_2COO^-$, known to be present in complex growth media, as a source of $m/z = +74$, cannot be ruled out and was further investigated. Specifically, Dulaney et al.⁴¹ isolated and purified betaine from yeast extract and showed that it contained $\sim 110 \mu\text{g}$ of betaine/g of yeast extract. The mass spectrum of trimethylglycine was collected and is shown in Figure 4. A large fragmentation peak at $m/z = +59$ corresponding to ${}^+N(CH_3)_3$ is observed. There are in addition small peaks at $m/z = +73$ and $+118$ corresponding to ${}^+N(CH_3)_2CH_2^+$ and ${}^+N(CH_3)_2CH_2COOH$. The BAMS mass spectrum of betaine was also examined in the presence of dipicolinic acid, which has a high UV absorption cross section at 266 nm ($\epsilon \sim 4000 \text{ L mol}^{-1} \text{ cm}^{-1}$) and constitutes up to 15% of the dry weight of a *Bacillus* spore. A 1:1 mixture of DPA and betaine was analyzed by BAMS. The resulting spectrum is shown in Figure 4 along with the spectrum of pure betaine standard. In addition to $m/z = +59$, the positive ion mass spectrum contains a large peak at $m/z = +74$. Additional peaks corresponding to ${}^+N(CH_3)_2CH_2COOH$ are observed at $m/z = +118$. This result shows that the DPA–betaine interaction produces a peak at $m/z = +74$. This is most likely formed by protonation of the anionic carbon site, ${}^+N(CH_3)_2CH_2^-$, resulting from decarboxylation of betaine. DPA-related peaks are observed in the negative spectra at $m/z = -166$, -122 , and -78 and correspond to the parent deprotonated ion and subsequent losses of one and two CO_2 groups. Control experiments with pure DPA aerosol standards did not produce a $m/z = +74$ peak as depicted in Figure 4. Based on the evidence of betaine in complex media and its fragmentation pattern in the presence of DPA, we believe that the $m/z = +74$ peak in the spore BAMS mass spectrum is ${}^+N(CH_3)_4$ from betaine. For the spore, the $m/z = +59$ peak observed in unlabeled media shifts by three mass units to $m/z = +62$ in the ^{13}C -labeled media, as is shown in Figures 1 and 2, and is consistent with an ${}^+N(CH_3)_3$ ion. A corresponding shift by one mass unit to $m/z = +60$ in the ^{15}N -labeled media is seen in some single spectra but attenuated in the average spectra shown in Figure 2. The $m/z = +59$ peak in

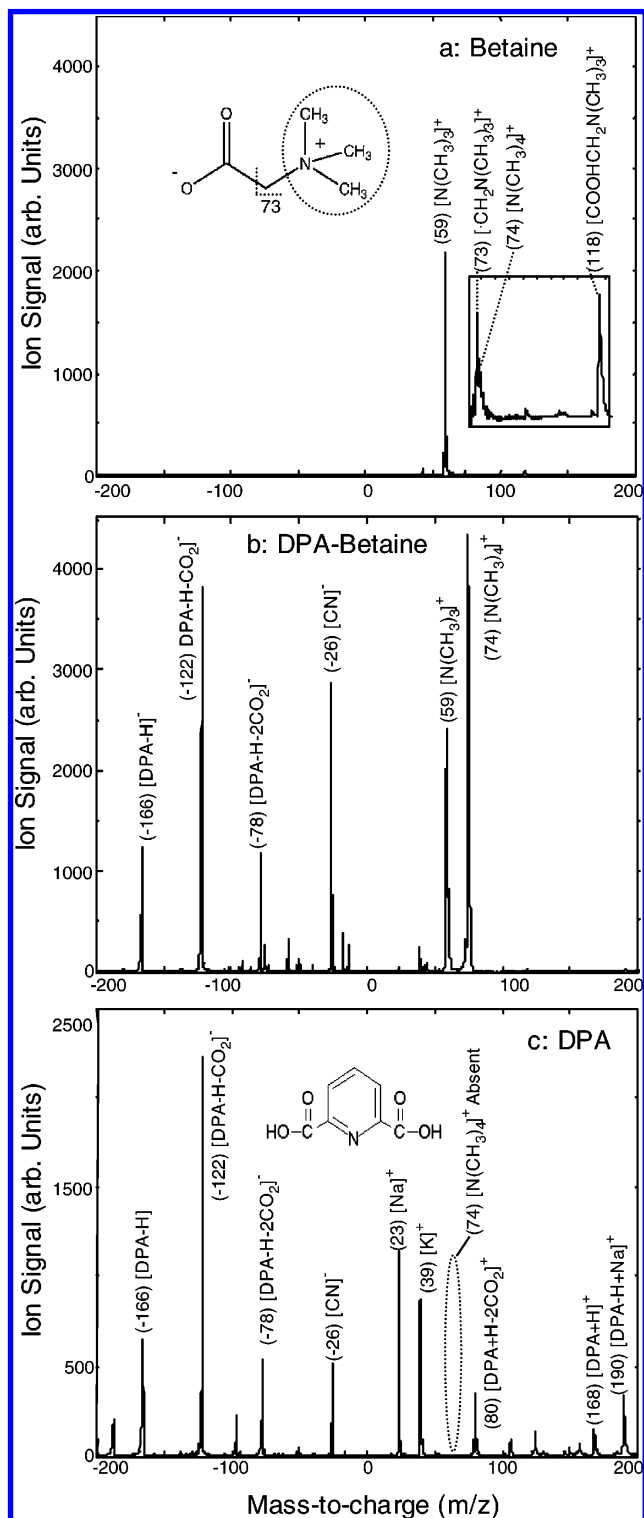


Figure 4. Dual polarity average mass spectra (200 spectra each) of (a) betaine, (b) betaine–dipicolinic acid (1:1 molar ratio), and (c) dipicolinic acid. All spectra were collected at 0.21 mJ average laser pulse energy. Note that in the presence of DPA a strong $m/z = +74$ peak is observed for betaine (betaine–DPA mixture, middle (b) figure).

the spore spectra is most likely ${}^+N(CH_3)_3$ and is consistent with the fragmentation of betaine in the presence of DPA. A small peak is also observed at $m/z = +118$ in the BAMS spore spectra for the unlabeled media. However, we could not determine if it is protonated betaine.

(40) Clejan, S.; Krulwich, T. A.; Mondrus, K. R.; Seto-Young, D. J. *Bacteriol.* **1986**, *168*, 334–340.

(41) Dulaney, E. L.; Dulaney, D. D.; Rickes, E. L. *Dev. Ind. Microbiol.* **1968**, *9*, 260–269.

CONCLUSION

All the prominent peaks in the BAMS mass spectrum of *B. atrophaeus* spore have been chemically assigned. These include prior assignments^{22,42} to dipicolinic acid and free amino acids in the spore BAMS mass spectra. A set of previously unidentified ion peaks at $m/z = -134$, -117 , -107 , and -90 that are present in the spore BAMS mass spectra are shown to be related to the fragmentation pattern of adenine-containing nucleotide structures. Additional contribution to $m/z = -90$ may arise from fragmentation of guanine as demonstrated with guanine-containing nucleotide standards. These results are consistent with the high purine nucleobase concentrations found inside *Bacillus* spores.

A clear identification of the spore BAMS mass spectrum allows us to evaluate the robustness of spore marker peaks. Specifically, $m/z = -173$ and $+74$ are marker peaks used¹⁶ to discriminate *B. atrophaeus* from *Bacillus thuringiensis* spore BAMS mass spectra. The association of $m/z = -146$ and $m/z = -173$ with glutamic acid and arginine for *B. atrophaeus* spore is consistent with their being the predominant free amino acids (present at equimolar concentration levels) in *B. subtilis* spores.³² However, unlike glutamic acid, arginine is found in only certain *Bacillus* spore species.³² In the case of *B. cereus* spores, free arginine is absent. To our knowledge similar data for *B. thuringiensis* spores is not available. We can only therefore suggest that the absence of a $m/z = -173$ peak in *B. thuringiensis* spore spectra¹⁶ is reflective of a lack of a free arginine pool in the *B. thuringiensis* spore.

The $m/z = +74$ ion for *B. atrophaeus* spores is also a differentiating marker peak from *B. thuringiensis* spores for certain growth media.¹⁶ The assignment obtained in our studies suggest it to be ${}^+N(CH_3)_4$, which can be derived from betaine. Betaine

can be transported into the cell via OpuA, OpuC, and OpuD osmoprotectant uptake systems for osmoregulation.⁴³ Furthermore, it can be synthesized via the GbsA and GbsB enzymes from exogenously provided choline taken up via the OpuB and OpuC ABC transporters. Further studies to probe the osmotic properties of *B. atrophaeus* and *B. thuringiensis* in high salt and glycine betaine-containing growth media are currently underway to better understand the factors controlling the presence of the fragmentation peak at $m/z = +74$ in *B. atrophaeus* and its absence in *B. thuringiensis*.

Our assignments of $m/z = -173$ and $+74$ therefore suggest that these peaks have to be used with caution for discrimination between *Bacillus* spore species with BAMS as they can be growth media dependent in the case of $m/z = +74$ and not unique to a single spore species in the case of $m/z = -173$. In order to overcome these limitations and obtain robust marker peak distinctions between *B. atrophaeus* and *B. thuringiensis* spores, higher m/z biomarkers that are potentially more specific need to be measured. Such studies are underway with our improved mass range BAMS instrument.

ACKNOWLEDGMENT

This work was performed under the auspices of the U.S. Department of Energy by University of California, Lawrence Livermore National Laboratory under Contract W-7405-ENG-48. This work was supported by the Lawrence Livermore National Laboratory through Laboratory Directed Research and Development Grant 02-ERD-002. This project was funded in part by the Technical Support Working Group of the Department of Defense.

(42) Fergenson, D. P.; Liu, D. Y.; Silva, P. J.; Prather, K. A. *Chemom. Intell. Lab. Syst.* **1997**, *37*, 197–203.

(43) Steil, L.; Hoffmann, T.; Budde, I.; Volker, U.; Bremer, E. *J. Bacteriol.* **2003**, *185*, 6358–6370.

Received for review November 17, 2004. Accepted March 11, 2005.

AC048298P